

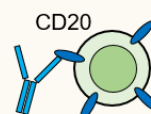
# Inhibition of HIF-1 $\alpha$ by Atorvastatin during $^{131}\text{I}$ -RTX Therapy in Burkitt's Lymphoma Model

Eun-Ho Kim, Hae Young Ko, A Ram Yu, Hyeongi Kim, Javeria Zaheer, Hyun Ji Kang, Young-Cheol Lim, Kyung Deuk Cho, Hyun-Yoo Joo, Min Kyoung Kang, Jae Jun Lee, Seung-Sook Lee, Hye Jin Kang, Sang Moo Lim and Jin Su Kim

Supplementary Materials:

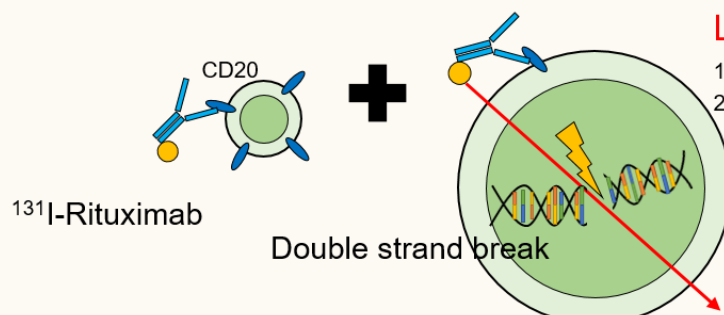
Rituximab therapy (immunotherapy)

Rituximab (anti-cd20)



$^{131}\text{I}$ -Rituximab therapy (Radio-immunotherapy) :

Synergistic effect of "antibody" + "radiation"





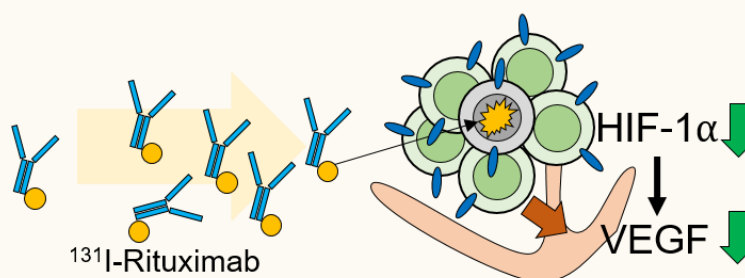
**Limitations:**

- 1) Radiation resistance under hypoxia
- 2) Limited transport of rituximab

$^{131}\text{I}$ -Rituximab therapy with atorvastatin (proposed method)

**Atorvastatin**

Penetration of rituximab   
Radio-resistance, Angiogenesis 



**Atorvastatin**

 **miR-346** 

**Figure S1.** Schematic of study design. RTX (anti CD20 antibody),  $^{131}\text{I}$ -RTX was used as a tool of targeted therapy.  $^{131}\text{I}$ -RTX provided synergistic effect of antibody and DNA double strand break due to  $^{131}\text{I}$ ; however, there were several limitations during  $^{131}\text{I}$ -RTX, indicating radiation resistance under hypoxia condition and limited transport of RTX. Therefore, in this present study, we proposed ATV combination study with  $^{131}\text{I}$ -RTX. We confirmed that HIF-1 $\alpha$  and VEGF were downregulated after ATV treatment.

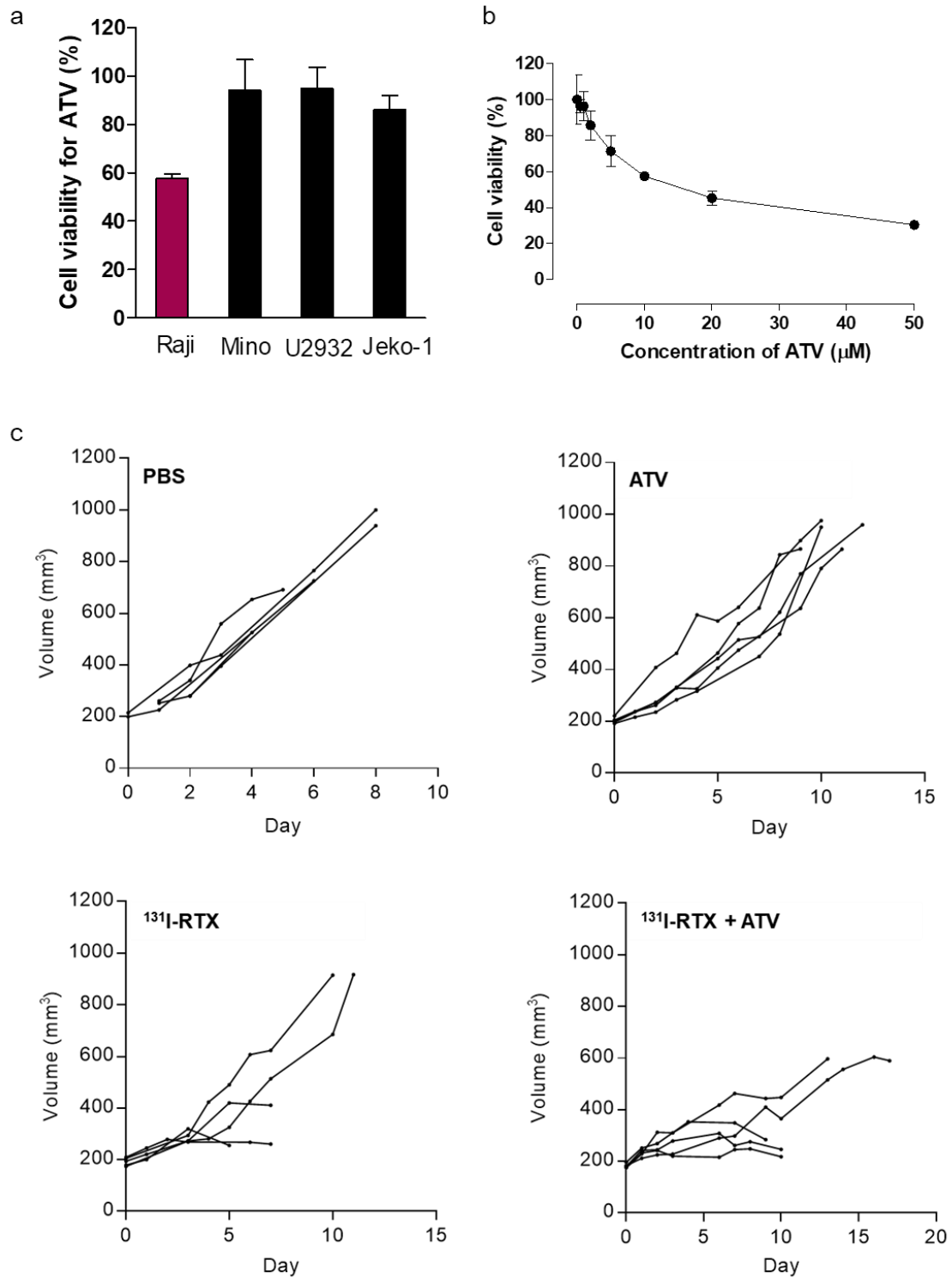


**Figure S2.** (a) After treatment with 10  $\mu$ M ATV or 5  $\mu$ g/mL RTX in Raji, Jeko-1, Mino, and U2932 lymphoma cells for 2 days, cell viability was determined by alamarBlue assay. (b) After treatment with various concentrations of ATV in Raji cells for 2 days, cell viability was determined by alamarBlue assay. The data were expressed as a percentage of the mean value of untreated control cells and the mean  $\pm$  SD from three independent experiments. (c) Tumor volume of each mouse

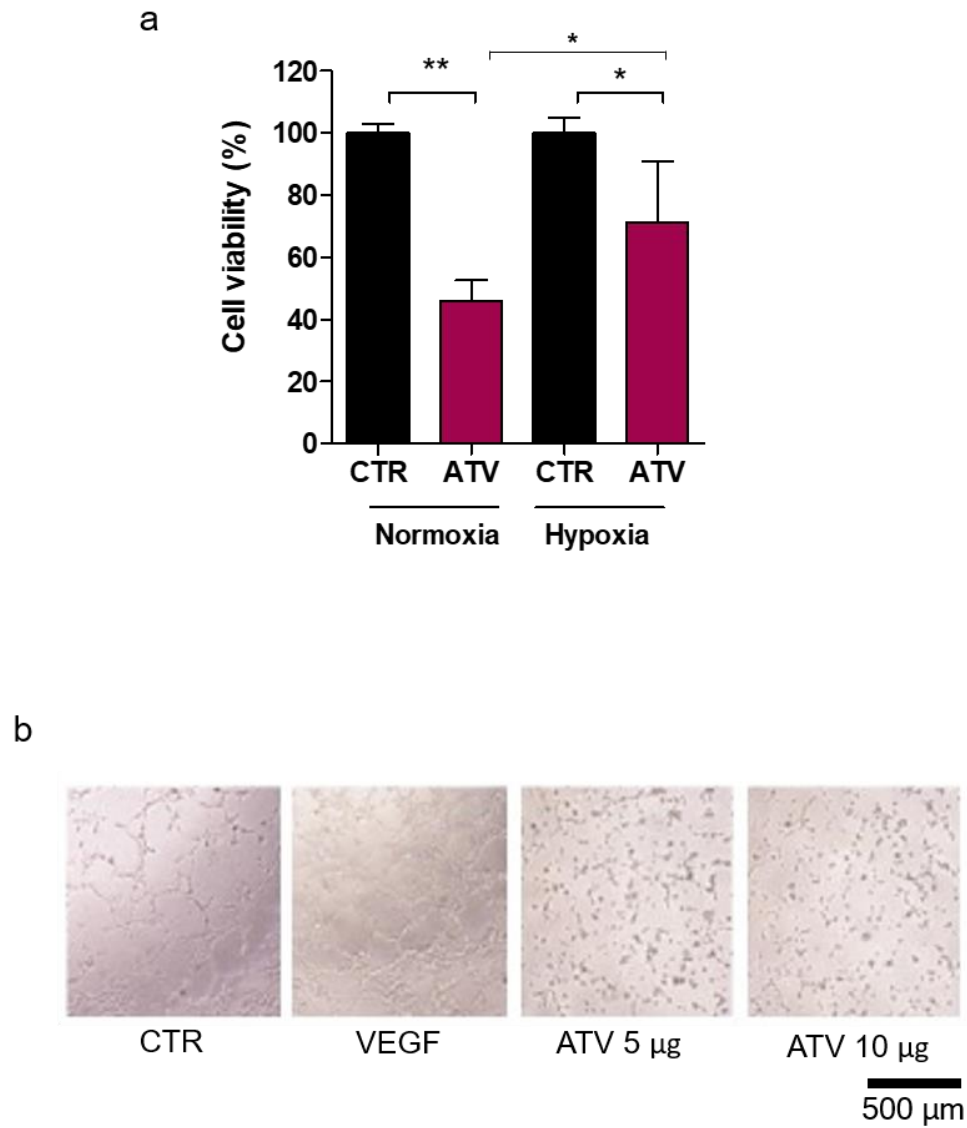


**Figure S3.** (a) ATV inhibited the viability of Raji cells, but hypoxia-induced Raji cells were less sensitive to ATV than the control. (b) The dysfunction in tube formation was significantly decreased after ATV treatment.

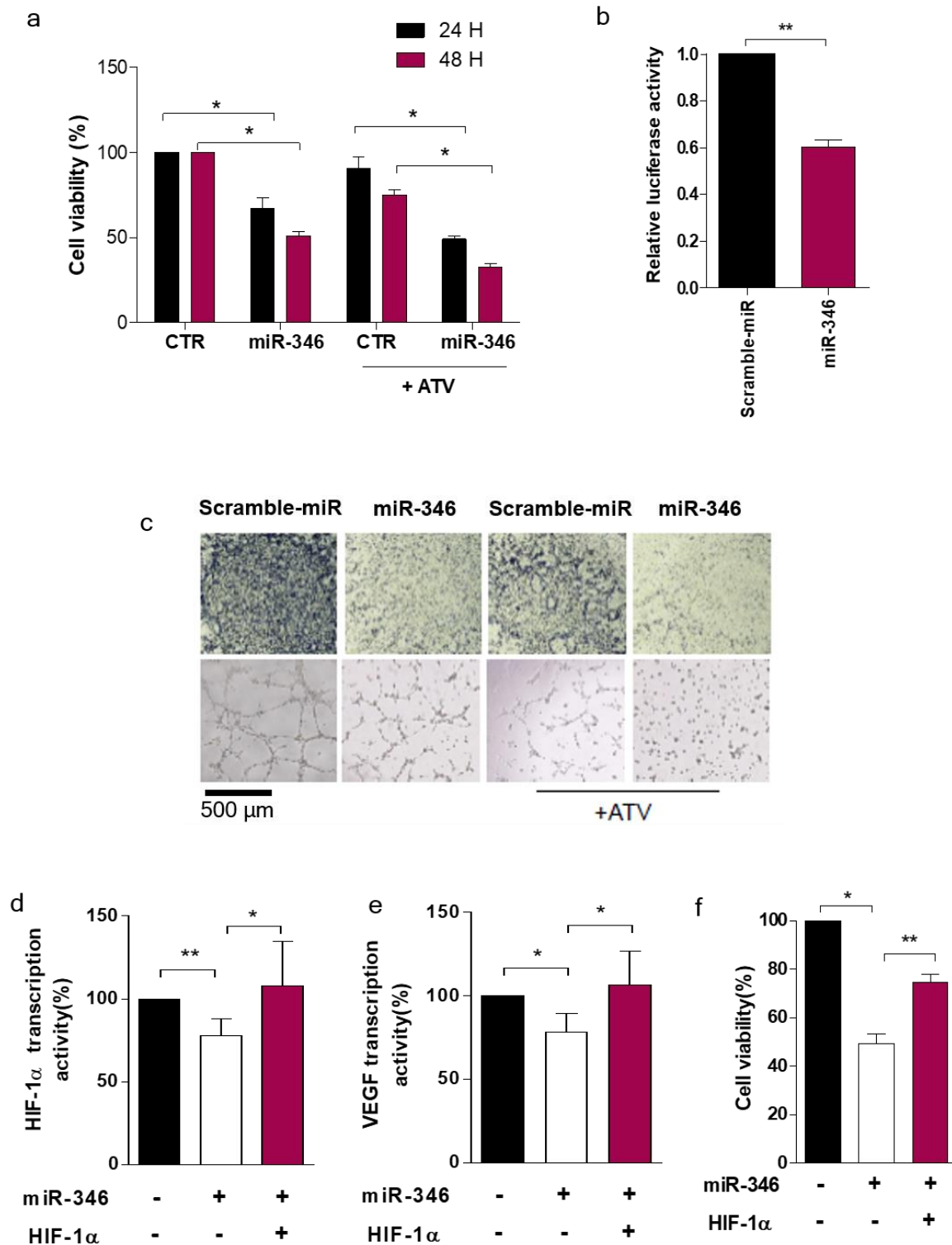


**Figure S4.** (a) Cell viability was determined after treatment with ATV and miR-346 transfection. The proliferation rate was measured by trypan blue exclusion method of cell viability. (b). The cells were cotransfected with either miR-346 or control mimics and 200 ng pGL3 reporter construct containing wild-type. The relative firefly luciferase activities normalized with Renilla luciferase were measured 48 h post transfection, and the results are plotted as percentage change over respective controls. (c). Tumor cell invasion and angiogenesis were assessed using Matrigel invasion assay and tube formation assay. Representative photomicrographs of in vitro tube formation. We cotransfected miR-346 mimic or mimic control with or without ATV treatment into Raji cells. (d) Transcriptional activity of HIF-1 $\alpha$  (\*\* $p$  < 0.005, \* $p$  < 0.05). (e). Transcriptional activity of VEGF (\*\* $p$  < 0.005, \* $p$  < 0.05). (f) Cell

viability: the decreased cell viability induced by miR-346 was restored by HIF-1 $\alpha^{\Delta 3'UTR}$  overexpression (\*\* $p < 0.005$ , \* $p < 0.05$ ).

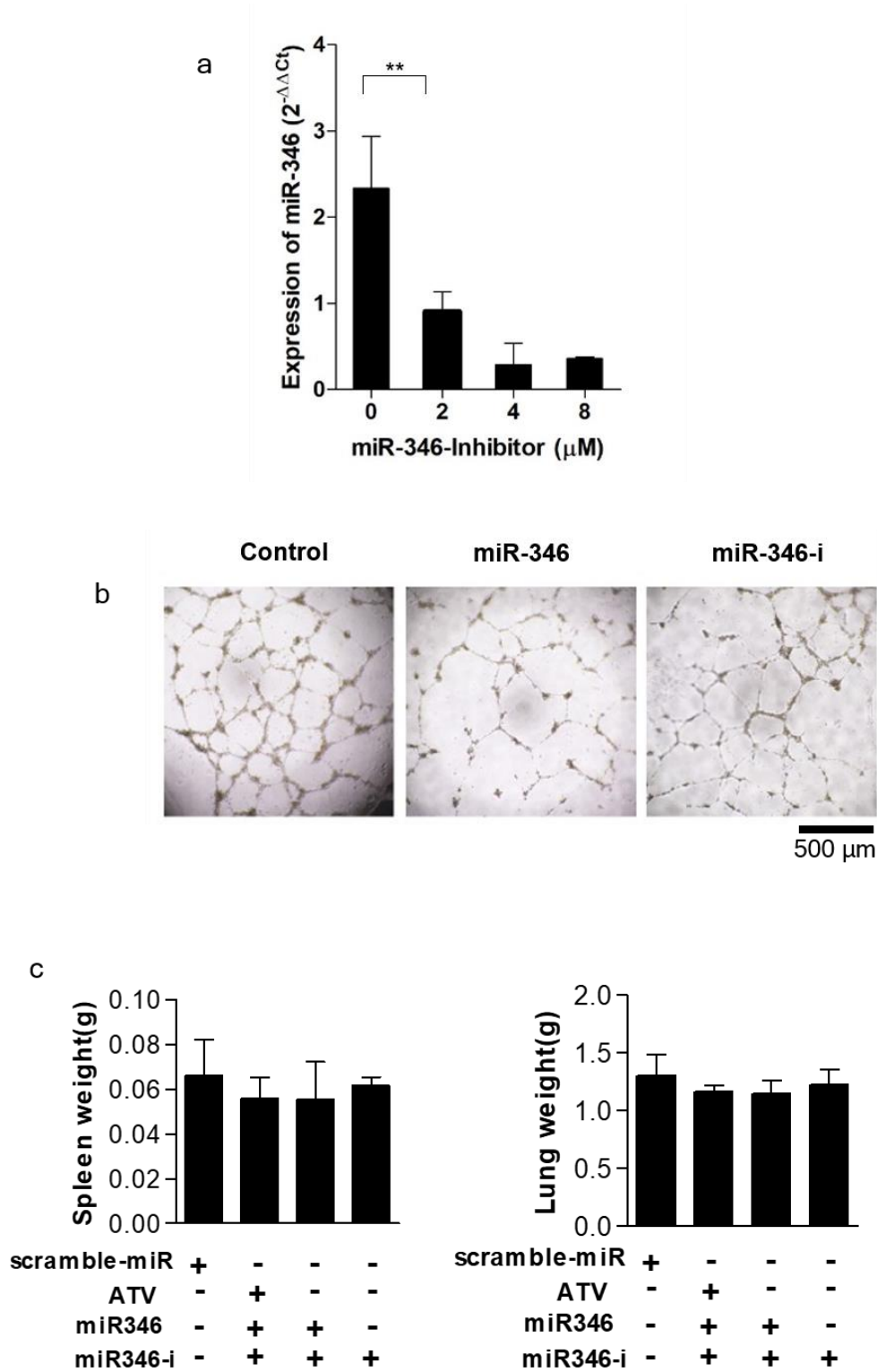


**Figure S5.** (a) The relative expression of miR-346 in Raji cells was analyzed according to the concentration of miR-346 inhibitor by qRT-PCR (\*\* $p < 0.005$ ). (b) Representative photomicrographs of in vitro tube formation after each treatment. (c) No weight change in the spleen and lung was detected, clearly indicating absence of acute toxicity.

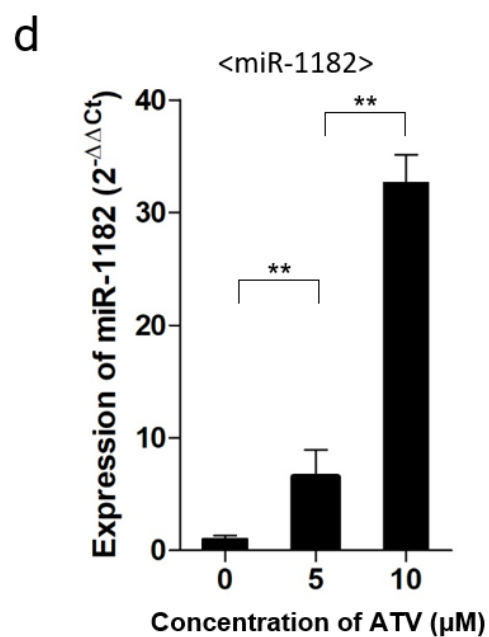
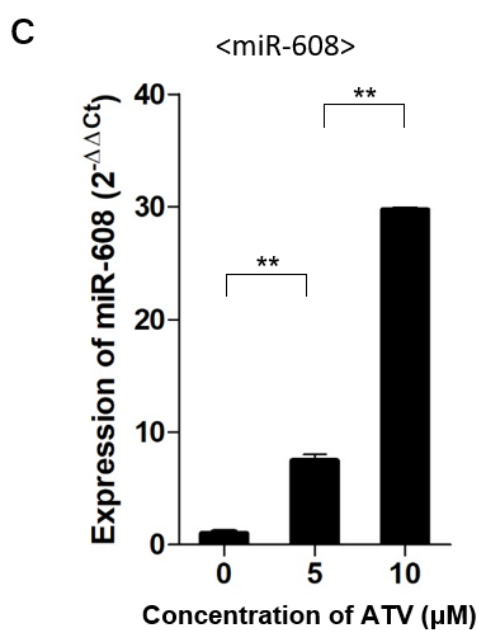
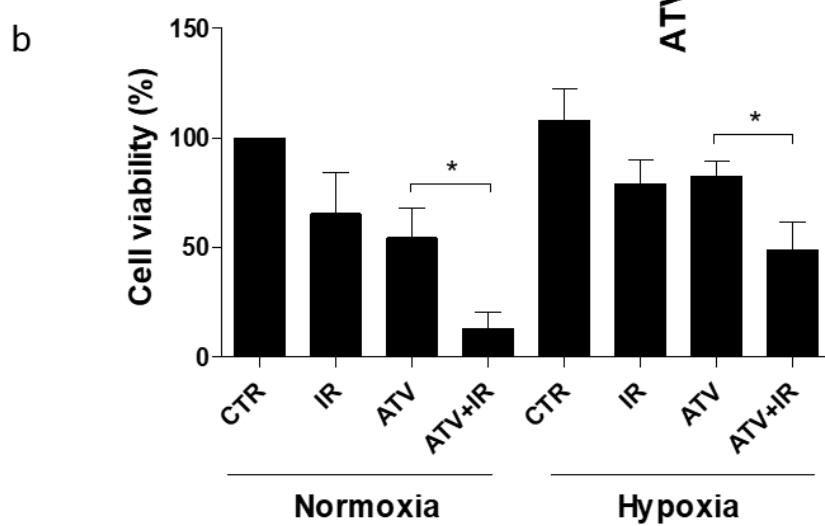
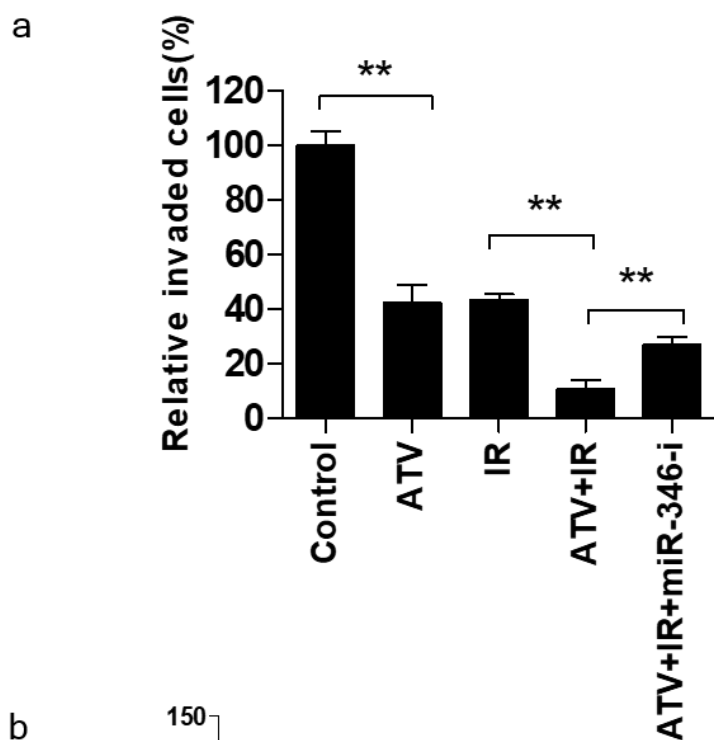


**Figure S6.** (a) Relative cell tumor invasion (%) by Matrigel invasion assay. (b) Cell viability: control and hypoxia-induced Raji cells received irradiation (6 Gy), atorvastatin treatment, or irradiation (6 Gy) + atorvastatin for 48 h. (c, d) Upregulated expression of miR-1182 and miR-608, which are related to inhibition of tumor growth and induction of cell death.

The whole western blot images of Figure 3, Figure 5a, Figure 6a

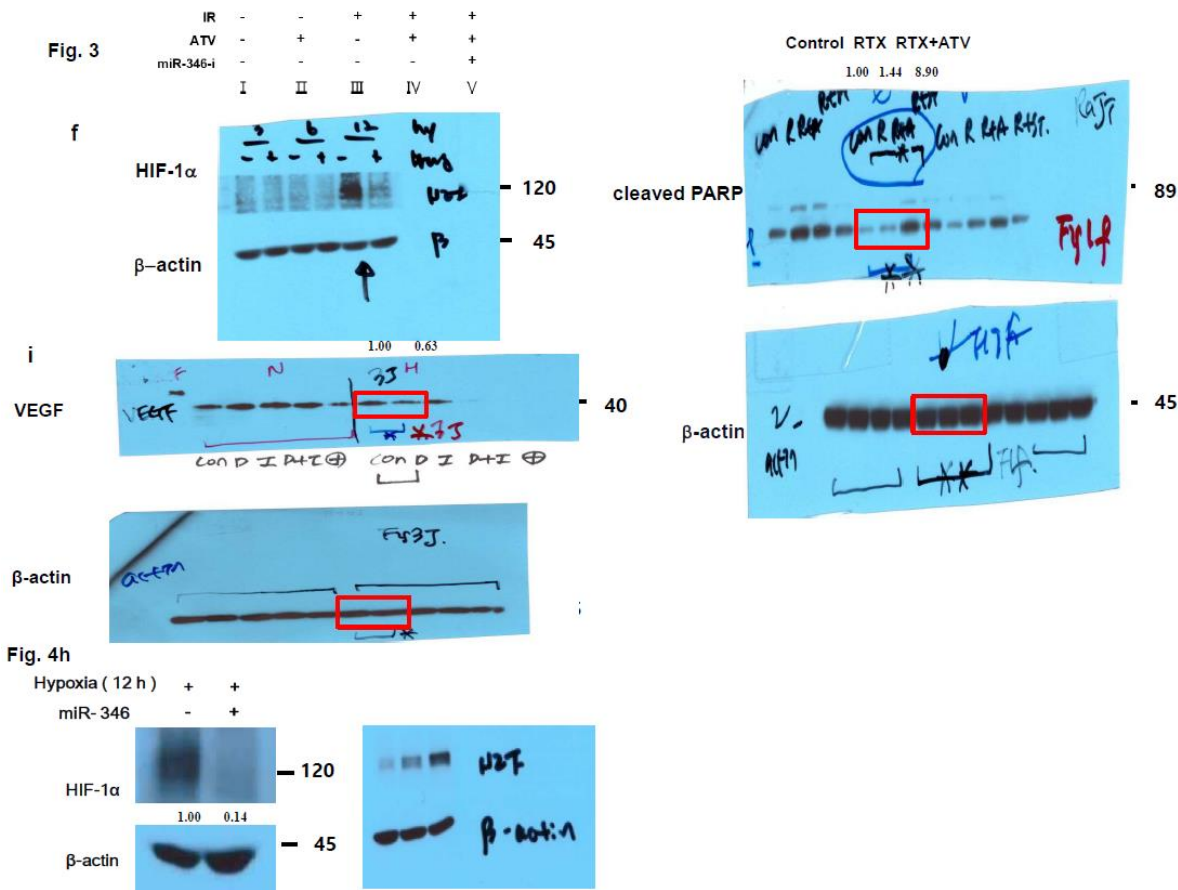




Fig. 5a

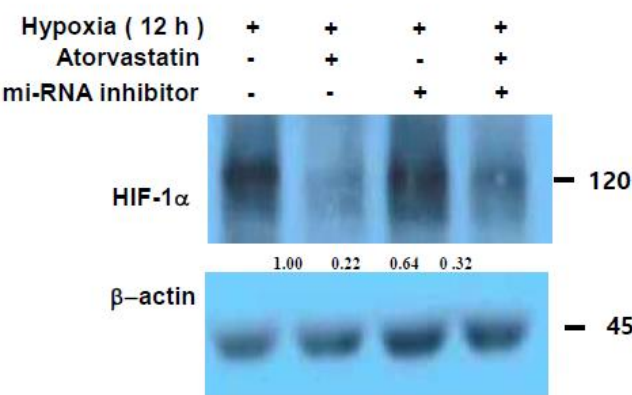


Fig. 5f

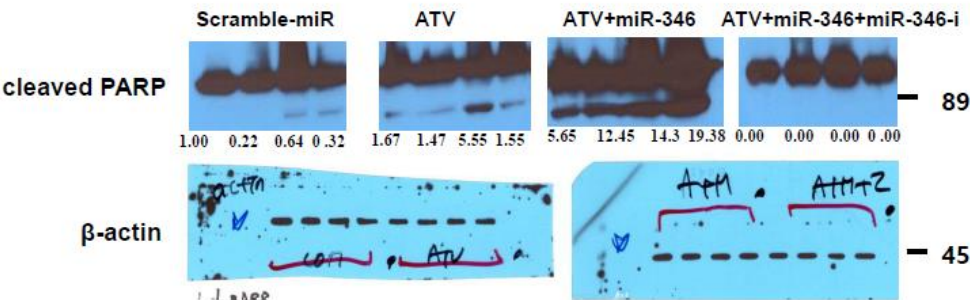


Fig. 6a

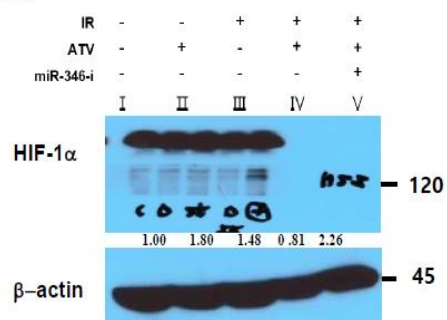


Fig. 6e

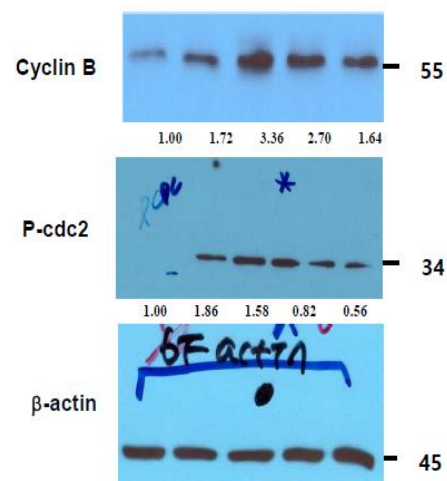
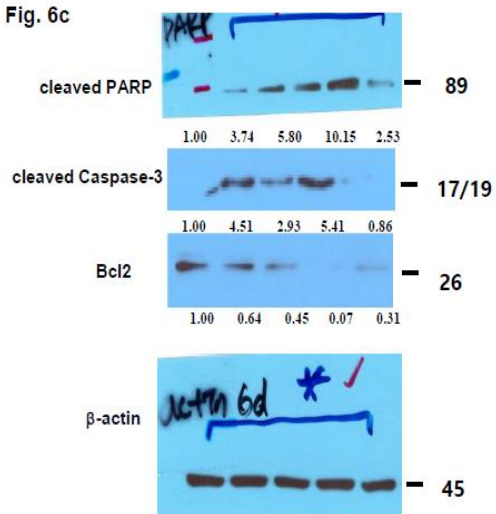


Fig. 6c



© 2020 by the authors. Submitted for possible open access publication under the terms and conditions of the Creative Commons Attribution (CC BY) license (<http://creativecommons.org/licenses/by/4.0/>).